

# Finite element simulation of traditional and earthquake resistant brick masonry building under shock loading

A. Joshua Daniel\* and R.N. Dubey<sup>a</sup>

*Department of Earthquake Engineering, Indian Institute of Technology Roorkee-247667, India*

*(Received May 5, 2014, Revised December 20, 2014, Accepted March 5, 2015)*

**Abstract.** Modelling and analysis of a brick masonry building involves uncertainties like modelling assumptions and properties of local material. Therefore, it is necessary to perform a calibration to evaluate the dynamic properties of the structure. The response of the finite element model is improved by predicting the parameter by performing linear dynamic analysis on experimental data by comparing the acceleration. Further, a nonlinear dynamic analysis was also performed comparing the roof acceleration and damage pattern of the structure obtained analytically with the test findings. The roof accelerations obtained analytically were in good agreement with experimental roof accelerations. The damage patterns observed analytically after every shock were almost similar to that of experimental observations. Damage pattern with amplification in roof acceleration exhibit the potentiality of earthquake resistant measures in brick masonry models.

**Keywords:** traditional brick masonry; earthquake resistant brick masonry; concrete damage plasticity; non-linear; acceleration; damage pattern

---

## 1. Introduction

Masonry is mainly a composite, anisotropic and a non-homogeneous material. The brickwork is a combination of bricks and mortar joints. The response of masonry subjected to loading depends on the properties of its brick, mortar and their interaction. Further, the response of masonry depends on the layout of bond and their interaction with other structural members. Modelling of masonry is a highly challenging process. Normally a high computation cost is associated with the intrinsic complexity of masonry (bricks connected by mortar joints) that requires a large number of degrees of freedom (Griordano *et al.* 2002), which usually excludes simplifications like rigid diaphragms and ideal connections which is applied in modelling of other kind of structures. Another reason for the complexity is that the material constitutive models which are not well defined, especially in the non-linear range.

As of now, numerical models have mainly been validated for an individual structural component. However, the validation of the entire building is still not available. Development of adequate techniques, which authenticate the numerical models, can be a major contribution to

---

\*Corresponding author, Post Graduate Student, E-mail: [ajoshdani@gmail.com](mailto:ajoshdani@gmail.com)

<sup>a</sup> Assistant Professor, E-mail: [rndubey84@gmail.com](mailto:rndubey84@gmail.com)

provide a powerful tool to assess and predict the performance of brick masonry structures. Until now, only a few studies refer to the analysis of masonry structures (Chavez *et al.* 2011, Oyarzo-Vera *et al.* 2009).

Based on the previous literature reviews it was revealed that the modulus of elasticity plays a vital role in representing the actual experimental behaviour of masonry. Further, the modulus of elasticity depends on other parameters like workmanship, quality of brick, quality of the mortar, thickness of the mortar joint, ambient condition and type of curing. In this regard, two main approaches namely, micro-modelling and macro-modelling are usually used for simulating the nonlinear behaviour of masonry structures. Micro-modelling includes the representation of bricks, mortar, and brick/mortar interfaces (Dhanaeskar *et al.* 1985, Zhuge *et al.* 1998) whereas, in macro-modelling there is no distinction between brick, mortar and brick/mortar interface (Chen *et al.* 2009, Page 1983). From literature review it is noted that one modelling strategy cannot be promoted over the other because different application fields exist for micro and macro models.

Micro-modelling gives a better understanding about the local behaviour of the masonry structure and this approach requires performing numerous experimental tests for calibrating the material properties. In macro-modelling, assuming masonry as a homogeneous material average stresses in the continuum masonry is related to the average strains in this modelling approach. Which is applicable when the structure is composed of solid walls with sufficiently large dimensions so that the stresses across or along length will be uniform. Macro-modelling gives a better understanding about the global behaviour of the masonry structure, where the interaction between brick and mortar are generally negligible (Lourenco *et al.* 1998). This approach is used to study the behaviour of large structures, where few experimental tests are sufficient for calibrating the material properties.

So, for an effective analysis, parametric study on Young's modulus will have to be carried out. During cyclic loading the masonry walls will be subjected to simultaneous in-plane and out-of-plane load (Rai *et al.* 2011). Individual validation on in-plane behaviour and out-of-plane behaviour of the material constitutive law, concrete damage plasticity (CDP) shows that it will be extremely effective under combined loading scenario. The same concrete damage plasticity (CDP) used by Rai *et al.* (2011) to study the non-linear behaviour of unreinforced masonry walls subjected to cyclic loading is used for this study. Further, a nonlinear dynamic analysis was also performed on the conventional brick masonry building. The problem statement of this study requires the explicit technique for analysis. This explicit technique does not require a fully assembled system's stiffness matrix; rather it solves the problem using the theory of dynamic wave propagation in solids. As iterations are not performed, much smaller increments of the applied load are required for the explicit technique to provide acceptable results and thus can simulate highly nonlinear events (Dhanasekar *et al.* 2007).

Dubey (2011) performed an experiment simultaneously on a traditional and an earthquake resistant brick masonry building on shock table facility available at the Department of Earthquake Engineering, IIT Roorkee. A total of eight shocks with intensity varying from 0.53g to 4.52g were applied at the base of the model. The corresponding acceleration obtained at roof after every shock was also recorded. In this study the first shock and its corresponding roof acceleration are being considered to calibrate of the model. We expect that this study will contribute to the improvement of calibration for analysis of the brick masonry buildings. Further, the effectiveness of this calibration will be verified by performing a non-linear dynamic analysis on conventional and an earthquake resistant brick masonry building by applying the base shock recorded during experimentation and by comparing the analytical roof acceleration and damage pattern with that of

the test findings.

## 2. Shock table testing

A low cost railway wagon shock table test facility is available at the Department of Earthquake Engineering, IIT Roorkee for dynamic tests on structural models up to 20 tons weight capacity. Shock table facility (Fig. 1) comprises of (i) 36 m long track or permanent way with pre-stressed concrete sleepers, (ii) shock table/ central wagon for carrying the models, (iii) one dead load wagon on each end for striking and rebound, (iv) end springs and (v) winch mechanism to pull the wagons. Shock table testing envisages testing of models under impulse type motion. One single shock imparts half - sine type of pulse to model base. Another wagon on the other side is used to take reaction; another half sine pulse can be imparted from the rebound. In this way one impact of end wagon can produce a series of half-sine pulses. The duration of the main shock varies between 0.1 to more than 0.5 sec and peak acceleration of shock could be in the range of 0.5 g to 10.0 g depending upon the stiffness of end springs and weight of striking wagon.

## 3. Model description

The traditional and an earthquake resistant brick masonry building, constructed on the shock table (Dubey 2011) were tested under the increasing intensity of the shock loading. As per IS: 13828 – 1993 & IS: 4326-1993 guidelines, to comprise an integral box action and to impart horizontal bending strength, the walls in earthquake resistant brick masonry model are tied together by horizontal seismic band at lintel level and vertical reinforcing bars are provided at corner and jamb steel are provided near the openings. The base acceleration as well as the roof acceleration was recorded. The plan and the elevation of the conventional and earthquake resistant brick masonry building are shown in Figs. 2 and 3.

## 4. Structural modelling

The physical model constructed on the shock table is modelled in ABAQUS. Macro modelling strategy is employed to model the masonry since the study is concerned with the global behaviour of the building. The walls, roof and lintel are modelled using a solid 8-noded linear hexahedral element with incompatible modes (C3D8I) (Oyarzo-Vera *et al.* 2009). Tie constraints are used to connect different structural members. The reinforcement is modelled using 2-noded, linear truss element (T3D2) and is embedded inside the respective material (Lee *et al.* 2007). During experimentation to have a rigidly fixed base condition, the wall of the buildings considered in this study are positioned along the shear key; which is been welded on the shock table (central wagon). The shock imparted on the central wagon makes it to displace along the direction of the track (Displacement is unrestrained). Similarly in FEM modeling displacement is unrestrained along the direction of shock loading and is restrained in all other directions. Fig. 4 show the meshed finite element model of conventional and earthquake resistant brick masonry building.

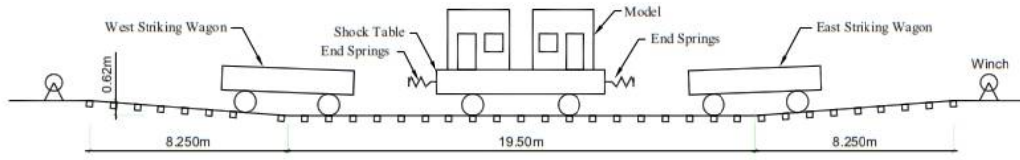


Fig. 1 Conventional brick masonry model

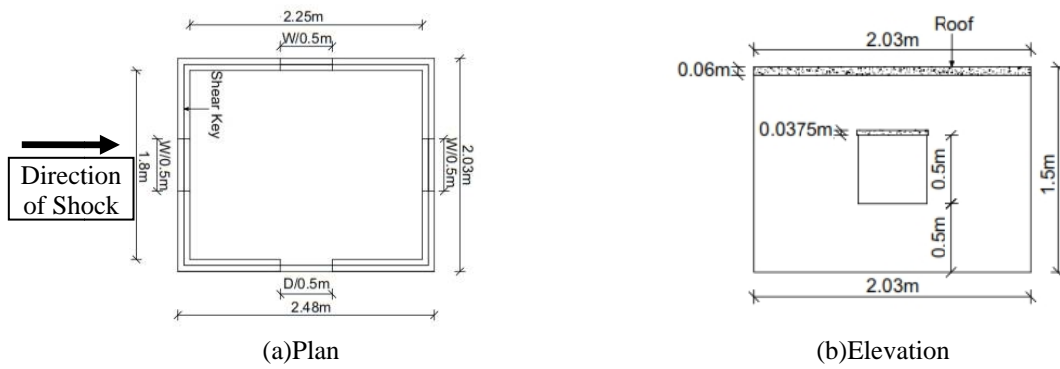


Fig. 2 Conventional brick masonry model

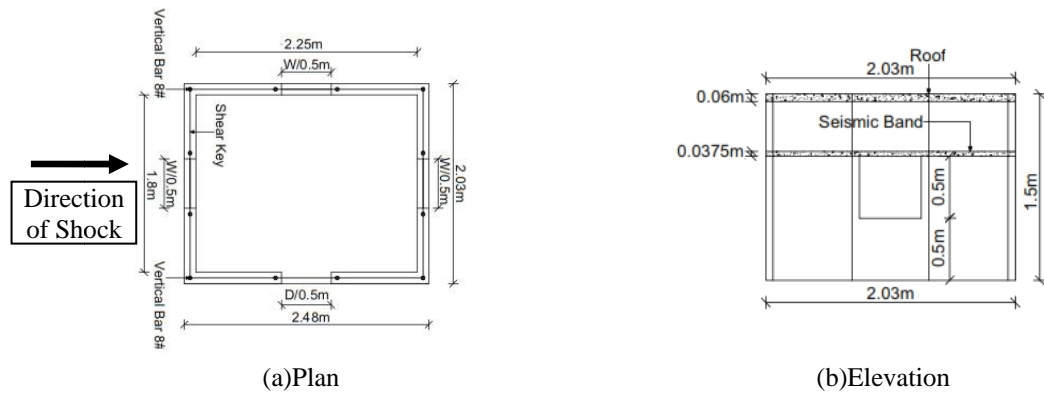


Fig. 3 Earthquake resistant brick masonry model



Fig. 4 Meshed finite element of brick masonry building

Table 1 Detail of parametric analysis for brick masonry building

Material	Trial	Young's Modulus N/m <sup>2</sup>	Base acceleration (in 'g')	Experimental roof acceleration (in 'g')	Analytical roof acceleration (in 'g')*
Conventional brick masonry building					
Masonry	1	2.3×10 <sup>9</sup>	0.53	0.59	0.57
	2	2.8×10 <sup>9</sup>	0.53	0.59	0.58
Earthquake resistant brick masonry building					
Masonry	1	2.3×10 <sup>9</sup>	0.53	0.61	0.57
	2	2.8×10 <sup>9</sup>	0.53	0.61	0.60

\*Analytical roof acceleration by retaining a constant: Density of Concrete = 2400Kg/m<sup>3</sup>; Young's modulus of Concrete = 1.94×10<sup>10</sup> N/m<sup>2</sup>; Poisson's ratio of Concrete = 0.2; Density of Steel = 7850 Kg/m<sup>3</sup>; Young's modulus of Steel = 2.00×10<sup>11</sup> N/m<sup>2</sup>; Poisson's ratio of Steel = 0.3; Density of Masonry = 1920 Kg/m<sup>3</sup>; Poisson's ratio of Masonry = 0.2

### 5. Result on parametric study

Masonry, Concrete and Steel are used in the model. Density, Poisson ratio and Young's modulus were the properties used in this parametric study. During experimentation, till second shock no crack was observed in these masonry buildings. It shows that the masonry is within the elastic limit. Hence the first shock is used to perform the parametric study. By applying the first shock at the base and by retaining constant value for all the materials except the Young's modulus of masonry, the roof acceleration obtained was compared with the experimental roof acceleration. A linear dynamic analysis was performed on both conventional and earthquake resistant brick masonry building and the Table 1 shows the corresponding detail of parametric analysis.

### 6. Material modelling

The seismic response is a cyclic process on all materials. The cyclic load has the influence on the material behaviour. Masonry is a brittle material with very low tensile strength. During uni-axial compression or tension test, modulus of elasticity is constant up to the yield point. The non-linear material properties help in understanding the material behaviour beyond the elastic range.

Concrete, masonry and rebar are the material used in the actual physical model. The metal plasticity in ABAQUS is used for recreating the nonlinear material response of rebar (DS Simulia 2011). The CDP in ABAQUS is used for replicating the nonlinear behaviour of concrete (DS Simulia 2011, Grecchi 2010 and Jankowiak *et al.* 2005). Similar to concrete, masonry is a brittle material with very low tensile strength. Therefore, CDP used for concrete is adopted for recreating the nonlinear behaviour of masonry.

### 6.1 Metal plasticity

For materials exhibiting ductile behaviour stress at yield of material is less than the elastic modulus of the material. The metal plasticity in ABAQUS uses the classical metal plasticity model with isotropic hardening. In isotropic hardening the yield surface changes size uniformly in all directions such that the yield stress increases (or decreases) in all directions as plastic straining occurs. In case of classical metal plasticity, strain softening/hardening followed by softening can be defined. The hardening behaviour in classical metal plasticity is defined by plastic strain value. The plastic strain is by a relation (DS Simulia 2011)

$$\varepsilon_{pl} = \varepsilon_0 - \frac{\sigma_0}{E} \quad (1)$$

Where  $E$  is the Young's Modulus,  $\varepsilon_{pl}$  is the plastic strain, and  $\varepsilon_0$  represent the yield strain corresponding to yield stress  $\sigma_0$ .

#### 6.1.1 Rebar

The steel grade of Fe250 is used for reinforcement. Fig. 5 shows the stress-strain curve (Pillai *et al.* 2010) with the corresponding stress-plastic strain curve. The other parameters used for steel in analysis are tabulated in Table 2. (Pillai *et al.* 2010, IS: 875 (Part-1)-1987, IS: 456 2000).

### 6.2 Concrete damage plasticity

Concrete and masonry are the brittle material with very low tensile strength. The Concrete Damage Plasticity Model (CDPM) in ABAQUS is used for replicating the nonlinear behaviour of concrete. The features of CDP are (DS Simulia 2011):

- Different yield strengths in tension and compression
- Softening behaviour in tension contrary to initial hardening followed by softening in compression
- Differential degradation of the elastic stiffness in tension and compression
- Stiffness recovery effects during cyclic loading

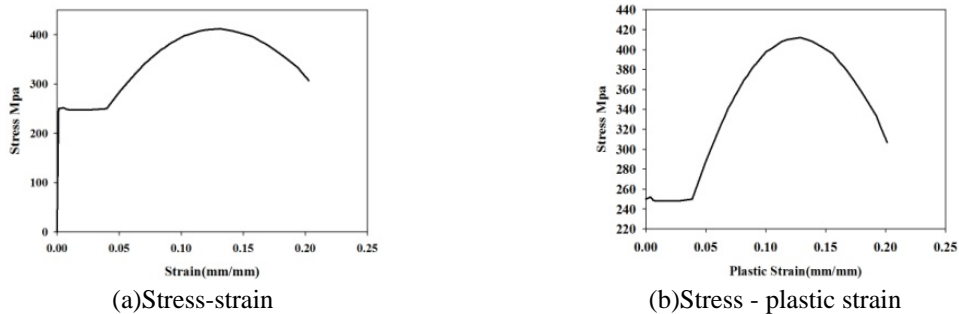


Fig. 5 Curve for Fe250 Curve

Table 2 Parameter for rebar

Property	Value
Density	7850 Kg/m <sup>3</sup>
Modulus of elasticity	2×10 <sup>11</sup> N/m <sup>2</sup>
Poisson ratio	0.3

Plasticity in CDP is generally defined as the unrecoverable deformation after all loads have been removed. Damage in material will be characterized by reduction of elastic constant. Both the decrease of unloading stiffness and unrecoverable deformation were observed in concrete compression clearly observed by (Maekawa *et al.* 2003 and Oshima *et al.* 1984). The CDPM in ABAQUS uses the concept of isotropic damage in combination with isotropic tensile and compression plasticity in order to represent the inelastic behaviour of concrete (DS Simulia 2011). The key aspects of CDP are the compressive behaviour, tension behaviour, compression damage variable, tension damage variable, yield criterion, hardening rule, softening rule and the flow rule.

Introduced and developed by (DS Simulia 2011, Lubliner *et al.* 1989, Hillerborg *et al.* 1976 and Lee *et al.* 1998) the constitutive equation of material with scalar isotropic damage takes the following form

$$\sigma_{ij} = D_{ijkl}^e (\varepsilon_{ij} - \varepsilon_{ij}^p) \times (1 - d) \tag{2}$$

Where,  $\sigma_{ij}$  is the stress tensor,  $d$  is the damage variable which characterizes the degradation of the elastic stiffness,  $D_{ijkl}^e$  is the initial (undamaged) elasticity,  $\varepsilon_{ij}$  and  $D_{ij}^p$  are the strain tensor and plastic strain tensor respectively. When the material is subjected to monotonic compression, above equation is simplified to

$$\sigma_1 = E_c (\varepsilon_1 - \varepsilon_1^p) \times (1 - d) \tag{3}$$

Where,  $\sigma_1$  and  $\varepsilon_1$  are the stress and strain of concrete in the loading direction respectively;  $\varepsilon_1^p$  is the plastic strain in the loading direction, and  $E_c$  is the initial elastic modulus of concrete. The effective stress is defined as

$$\bar{\sigma}_1 = \frac{\sigma_1}{1 - d} \tag{3}$$

In this study, compressive behaviour, tension behaviour, compression damage variable and tension damage variable were calculated for the respective material from the appropriate stress-strain curve. Other key aspects like the yield criterion, hardening rule, softening rule and the flow rule are adopted from previous literature review. CDP has the feature of enabling different yield strength in compression and tension. Fig. 6(a) shows the Stress-strain for concrete in compression. Fig. 6(b) shows the Stress-strain for concrete in tension. Fig. 9(a) shows the Stress-strain for masonry in compression. Fig. 9(b) shows the Stress-strain for masonry in tension. The shock loading is applied at the base of the model. When the stresses in the materials are within the Elastic limit, strain will be proportional to stress, hence upon unloading material will recover its original shape. When the stress in the materials exceed Elastic limit, the material will undergo permanent

deformation. When compression force is applied on the materials and upon exceeding its Elastic limit, the material endures crushing (Hence the graph (i.e., 7(a) and 10(a)) is between stress and crushing strain). On the other hand, when tensile force is applied on the materials and upon exceeding its Elastic limit the material endures cracking (Hence the graph (i.e., 7(b) and 10(b)) is between stress and cracking strain). CDP has the feature of enabling differential degradation of the elastic stiffness in tension and compression. For each variation in crushing strain (i.e., 7(a) and 10(a)) and cracking strain (i.e., 7(b) and 10(b)), the corresponding damage variable is shown by the Fig. 8 and 11.

6.2.1 Concrete

The concrete used for lintel and R.C slab is of grade M15. The characteristic compression strength,  $f_{ck}$  (IS: 456 – 2000) for M15 grade is 15Mpa. The stress-strain curve for concrete in compression is developed from an empirical relation (Hu *et al.* 2004). The maximum stress will be reached at a strain approximately equal to 0.002 (IS: 456 – 2000). The strain at which the failure of concrete occurs is taken as 0.005 (Pillai *et al.* 2010). The stress-strain curve for concrete in tension is developed from an empirical relation (Vecchio 1990). The flexural strength of concrete is calculated based on the formula  $0.7\sqrt{f_{ck}}$  (IS: 456 – 2000). The limiting tensile strain of concrete is 0.0001 (Pillai *et al.* 2010). Fig. 6 shows the stress-strain curve for concrete in compression and tension. Fig. 7 shows the behaviour of concrete in compression and tension. The compression and tension damage for concrete is shown in Fig. 8. The other parameters used for concrete in analysis are tabulated in Table 3. (Jankowiak 2005).

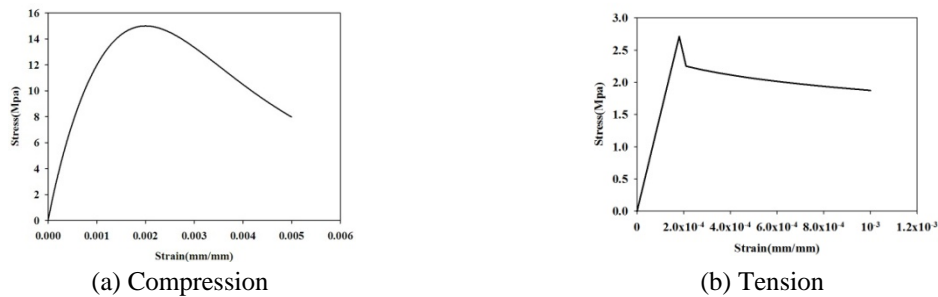


Fig. 6 Stress-strain for concrete

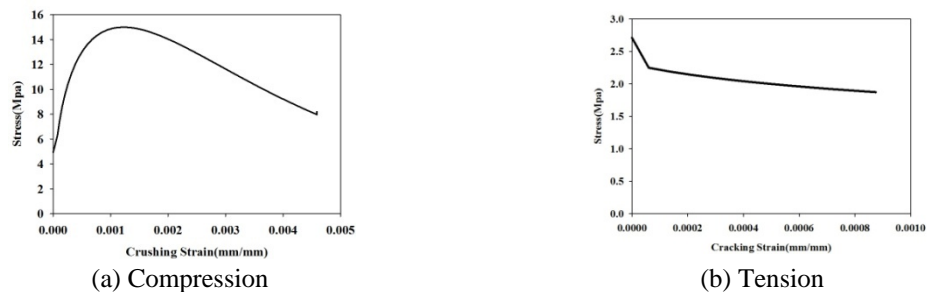


Fig. 7 Compression behaviour for concrete

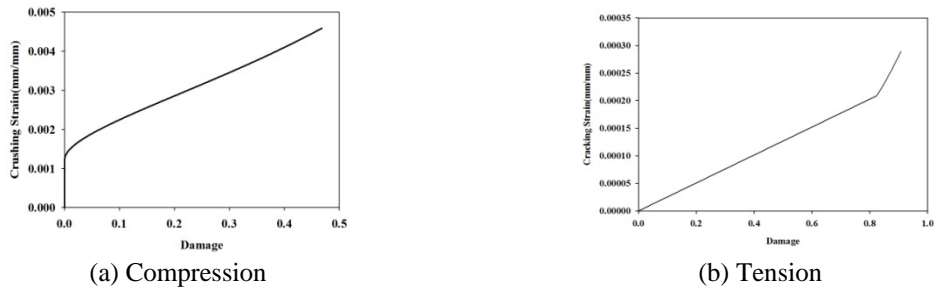


Fig. 8 Damage of concrete

### 6.2.2 Masonry

The compression strength of masonry prism used in this study is 4.1 Mpa (Kaushik *et al.* 2006). The Stress strain curve for masonry in compression has been developed using tri-linear model (Kaushik *et al.* 2006). The tensile strength of masonry used in this study is 0.28 MPa (Nateghi *et al.* 2008). The stress-strain curve for masonry in tension is developed from empirical relation (Chen *et al.* 2008) is adopted for this model. Fig. 9 shows the stress-strain curve for masonry in compression and tension. Fig. 10 shows the behaviour of masonry in compression and tension. The compression and tension damage for masonry is shown in Fig. 11. The other parameters used for masonry in analysis are tabulated in Table 3 (Rai *et al.* 2011).

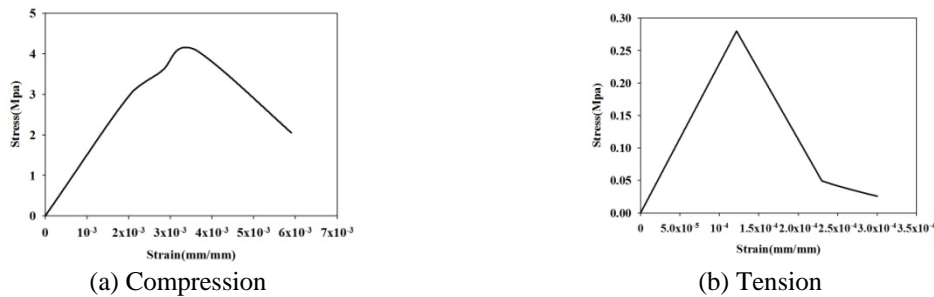


Fig. 9 Stress-strain for masonry

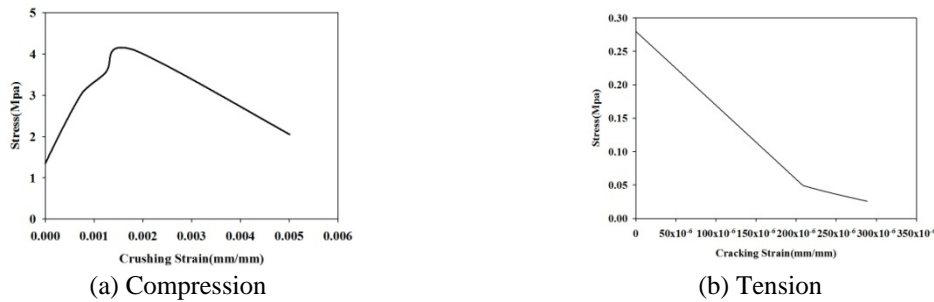


Fig. 10 Compression behaviour for masonry

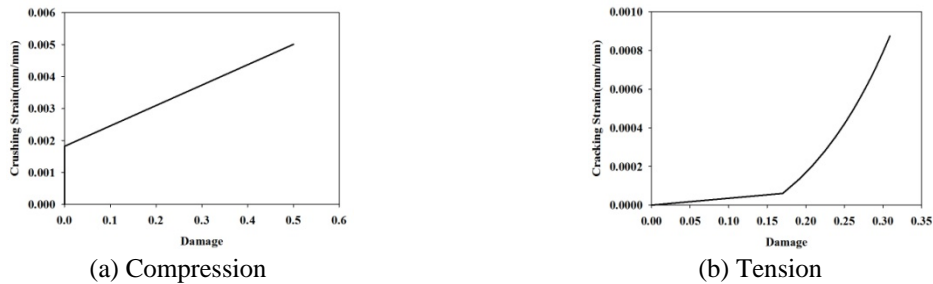


Fig. 11 Damage of masonry

Table 3 Parameter for concrete and masonry

Property	Concrete Value	Masonry Value
Density	2400 Kg/m <sup>3</sup>	1920 Kg/m <sup>3</sup>
Modulus of elasticity	1.94×10 <sup>10</sup> N/m <sup>2</sup>	2.8×10 <sup>9</sup> N/m <sup>2</sup>
Poisson ratio	0.2	0.2
Dilation angle	38°	30°
Flow potential eccentricity	0.1	0.1
Ratio of initial compressive yield stress to initial uni-axial compressive yield stress	1.16	1.16
Ratio of second stress invariant	0.667	0.667
Viscosity parameter	0	0

## 7. Observation

The conventional and earthquake resistant brick masonry building modelled in ABAQUS was subjected to a gradually increasing intensity of shock loading. During experimentation on the actual physical model, the conventional building collapses during the fifth shock while the earthquake resistant building withstood all the eight shocks which is been applied on the model.

### 7.1 Damage

During the experiment, the shock was applied along east west direction. The same is being simulated analytically, and it was observed that until third shock, there was no visible damage on the traditional brick masonry model. The same situation has also been observed during experimentation. Fig. 12 shows the development of stress near the corners of the opening.

The walls in the physical model are damaged during the fourth shock. A similar situation has been observed during simulation. Fig. 13 shows the damage of the bending wall on west side. Fig. 14 shows the damage of south shear wall. Fig. 15 shows the damage of the bending wall on east

side. Fig. 16 shows the damage of north shear wall. The traditional brick masonry model withstood five shocks and the Fig. 17 show corresponding damage of the wall during the fifth shock.

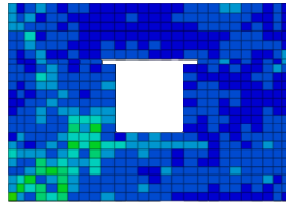
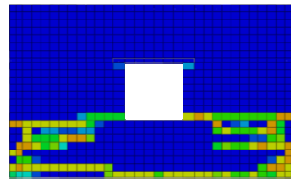


Fig. 12 Stress developed in corner of opening during shock 3



(a) Experimental

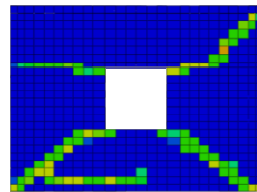


(b) Analytical

Fig. 13 Comparison of damage on west side wall after fourth shock (Horizontal bending crack at the foundation level and near the window opening spreading up to the corner)



(a) Experimental

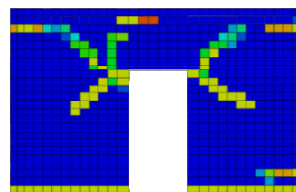


(b) Analytical

Fig. 14 Comparison of damage on south side wall after fourth shock (Diagonal shear cracks starting from window opening and horizontal cracks at the base of the walls and from the corner of the window opening)



(a) Experimental



(b) Analytical

Fig. 15 Comparison of damage on east side wall after fourth shock (Diagonal crack starting from the door opening spreading up to the corner)



Fig. 16 Comparison of damage on north side wall after fourth shock (Diagonal shear cracks starting from window opening and horizontal cracks at the base of the walls and from the corner of the window opening)



Fig. 17 Comparison of damage on north side wall after fifth shock (Wide and diagonal shear crack originating from window openings and spreading to the corner)

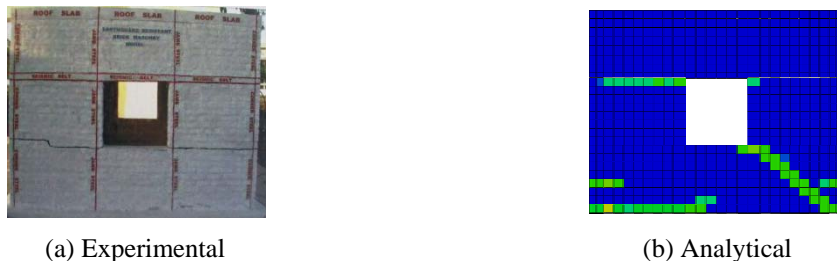


Fig. 18 Comparison of damage on south side wall after sixth shock (Horizontal cracks originating from the window opening appeared on the southern shear walls)

Simultaneously, experimentation on earthquake resistant brick masonry model shows that until fifth shock, there was no visible damage on the masonry building. The same situation has also been observed during stimulation. The walls in the physical model are damaged during the sixth shock. A similar situation has been observed during simulation. Fig. 18 shows the minor damage on the south shear wall after sixth shock. Figs. 19 and 20 shows the respective damages on north shear wall after seventh and eighth shocks. The earthquake resistant brick masonry model withstood all the eight shock. The damage pattern obtained analytically were quiet similar to that of the experiment.



Fig. 19 Comparison of damage on north side wall after seventh shock (Diagonal shear crack were also observed at the corners of the walls)



Fig. 20 Comparison of damage on north side wall after eight shock (Several diagonal shear cracks were also observed at north shear wall)

### 7.2 Acceleration

The acceleration recorded at the base during actual physical testing is applied at the base of the analytical model. The roof acceleration thus obtained is compared with the experimental roof acceleration. Figs. 21 to 28 show the comparison of base acceleration applied at the base of the model recorded during experiment, with the corresponding analytically obtained roof acceleration for the traditional and earthquake resistant brick masonry building. Table 4 shows the peak absolute base acceleration of each shock with corresponding experimental as well as analytical roof acceleration for both the building. Earthquake resistant model was stiffer than the traditional model and that is why the amplification was more in earthquake resistant model.

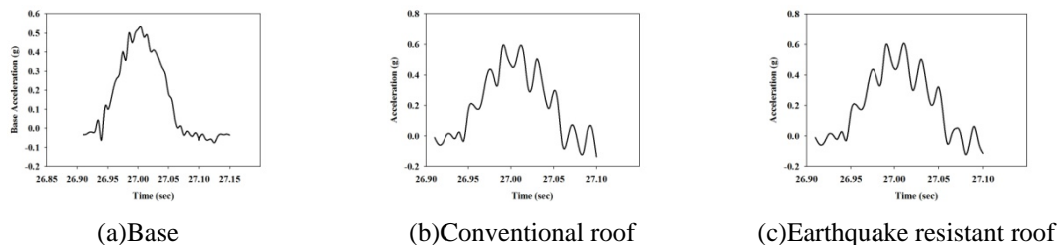
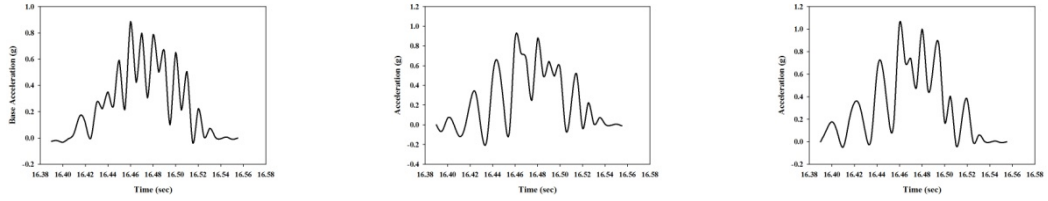
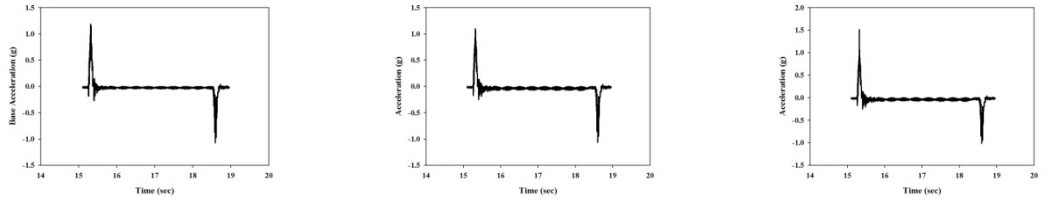


Fig. 21 Input acceleration at base and estimated response at roof of shock 1



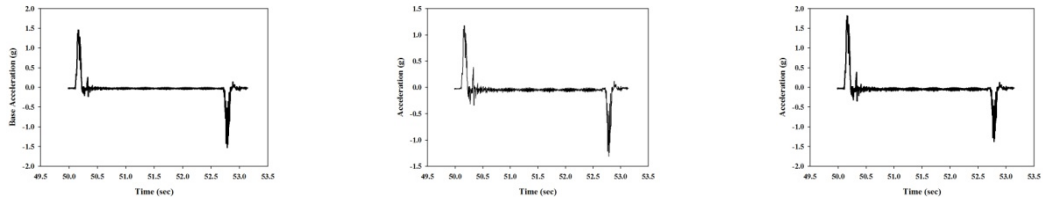
(a)Base (b)Conventional roof (c)Earthquake resistant roof

Fig. 22 Input acceleration at base and estimated response at roof of shock 2



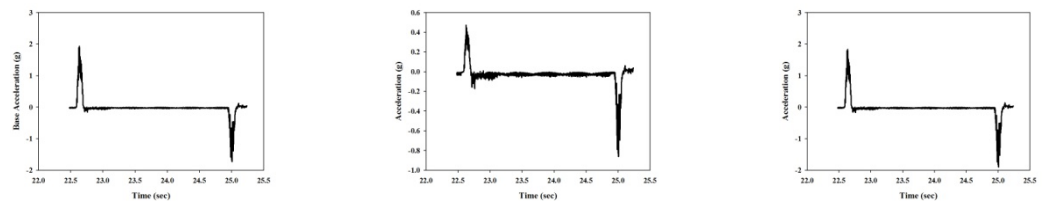
(a)Base (b)Conventional roof (c)Earthquake resistant roof

Fig. 23 Input acceleration at base and estimated response at roof of shock 3



(a)Base (b)Conventional roof (c)Earthquake resistant roof

Fig. 24 Input acceleration at base and estimated response at roof of shock 4



(a)Base (b)Conventional roof (c)Earthquake resistant roof

Fig. 25 Input acceleration at base and estimated response at roof of shock 5



Fig. 26 Input acceleration at base and estimated response at roof of shock 6



Fig. 27 Input acceleration at base and estimated response at roof of shock 7

Table 4 Comparison of roof acceleration for conventional model and earthquake resistant model

Shock	Peak absolute base acceleration (in 'g')		Experimental peak absolute horizontal roof acceleration (in 'g')		Analytical peak absolute horizontal roof acceleration (in 'g')	
	Loading pulse	Rebound pulse	Loading pulse	Rebound pulse	Loading pulse	Rebound pulse
<b>Traditional brick masonry building</b>						
Shock 1	0.53	---	0.59	---	0.58	---
Shock 2	0.88	---	0.91	---	0.88	---
Shock 3	1.18	1.05	1.14	1.10	1.10	1.05
Shock 4	1.45	1.51	1.24	1.38	1.18	1.30
Shock 5	1.93	1.62	0.51	0.88	0.44	0.80
<b>Earthquake resistant brick masonry building</b>						
Shock 1	0.53	---	0.61	---	0.60	---
Shock 2	0.88	---	1.09	---	1.05	---
Shock 3	1.18	1.05	1.55	1.03	1.51	0.99
Shock 4	1.45	1.51	1.88	1.44	1.81	1.35
Shock 5	1.93	1.62	2.02	1.84	1.83	1.75
Shock 6	2.73	2.18	2.90	2.62	2.70	2.51
Shock 7	3.38	3.35	3.85	3.62	3.55	3.42
Shock 8	4.52	4.05	4.59	4.14	4.50	3.79

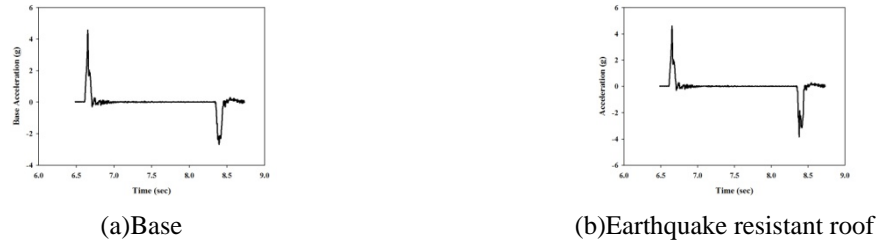


Fig. 28 Input acceleration at base and estimated response at roof of shock 8

## 8. Conclusions

Modelling and analysis of brick masonry building involves uncertainties like modelling assumptions and the properties of local material. The properties of local material include numerous other parameters like workmanship, quality of brick, quality of the mortar, thickness of the mortar joint, ambient condition and type of curing. Since the intension of this study, regards the global behaviour of masonry, macro-modelling approach is used. Which itself involves uncertainties like modelling assumptions and the properties of local material. To overcome these uncertainties a parametric study was performed to estimate the dynamic property comparing the roof acceleration of the first shock. Further, a nonlinear dynamic analysis was also performed comparing the roof acceleration and damage pattern of the structure obtained analytically with that of the experimental observation. The conclusions drawn from the foregoing study are summarized below

- The roof accelerations obtained analytically were in good agreement with experimental roof accelerations. The variation in the roof accelerations were 16% and 13% for traditional and earthquake resistant models respectively.
- No damage was observed both in analytical model as well as during experimentation till third shock. But the development of stress near the corner of the opening is same as expected during the third shock.
- In case of earthquake resistant brick masonry model no damage was observed both in analytical model as well as during experimentation till fifth shock.
- Experimental observation shows the real behaviour of the structure. Hence, the crack propagation and the damage pattern observed experimentally in both the building after every shock were in good agreement with that of the analytical observations.
- During experimental investigation it was observed that the traditional brick masonry model was completely collapsed after sixth shock. But for the same shock, during simulation the conventional model withstood load, higher than its capacity. This is due to the limitations of concrete damaged plasticity.

## Acknowledgments

The authors are indebted to Head, Department of Earthquake Engineering, Indian Institute of Technology, Roorkee for providing facilities to carry out the analytical work reported in this paper.

First author acknowledges with thanks to the research fellowship received from the Ministry of Human Resource Development, Government of India.

## References

- Chavez, M. and Meli, R. (2011), "Shaking table testing and numerical simulation of the seismic response of a typical Mexican colonial temple", *Earthq. Eng. Struct. D.*, **41**(2), 233-253.
- Chen, S.Y., Moon, F.L. and Yi, T.A. (2009), "Macroelement for the nonlinear analysis of in-plane unreinforced masonry piers", *Eng. Struct.*, **30**(8), 2242-2245.
- Chen, Y., Ashour, A.F. and Garrity, S.W. (2008) "Moment/thrust interaction diagrams for reinforced masonry sections", *Constr. Build.Mater.*, **22**(5), 763-770.
- Dhanaeskar, M., Kleeman, P.W. and Page, A.W. (1985), "Biaxial stress-strain relations for brick masonry", *J. Struct. Div.*, **111**(5), 1085-110.
- Dhanasekar, M. and Haider, W. (2007), "Explicit finite element analysis of lightly reinforced masonry shear wall", *Comput. Struct.*, **86**, 15-26.
- Dubey, R. (2011), *Experimental studies to verify the efficacy of earthquake resistance measure in masonry structures*, Ph.D. thesis, Earthquake Engineering Department, Indian Institute of Technology Roorkee, Roorkee, India.
- Giordano, A., Mele, E. and De Luca, A. (2002), "Modelling of historical masonry structures: Comparison of different approaches through a case study", *Eng. Struct.*, **24**(8), 1057-1069.
- Grecchi, G. (2010), *Material and structural behavior of masonry: simulation with a commercial code Laurea*, Thesis, University of Pavia, Lombardy, Italy.
- Hillerborg, A., Modeer, M. and Petersson, P.E. (1976), "Analysis of crack formation and crack growth in concrete by means of fracture mechanics and finite elements", *Cement Concrete Res.*, **6**, 773-782.
- Hu, T.H., Lin, F.M. and Jan, Y.Y. (2004) "Nonlinear finite element analysis of reinforced concrete beams strengthened by fiber-reinforced plastics", *Compos. Struct.*, **63**(3-4), 271-281.
- IS: 875 (Part 1), (1987), *Code of practice for design loads (other than earthquake) for building and structures*, Bureau of Indian Standard, New Delhi, India.
- IS: 13828 (1993), *Improving earthquake resistance of low strength masonry building – Guidelines*, Bureau of Indian Standard, New Delhi, India.
- IS: 4326 (1993), *Indian standard code of practice for earthquake resistant design and construction of buildings*, Bureau of Indian Standard, New Delhi, India.
- IS: 456 (2000), *Plain and reinforced concrete - Code of practice*, Bureau of Indian Standard, New Delhi, India.
- Jankowiak, T. and Lodygowski, T. (2005), "Identification of parameters of concrete damage plasticity constitutive model", *Found. Civil Environ. Eng.*, **6**, 53-69.
- Kaushik, H.B., Rai, D.C. and Jain, S.K. (2007), "Stress-strain characteristics of clay brick masonry under uniaxial compression", *J. Struct. Eng. - ASCE*, **19**(9), 728-739.
- Lee, H.K., Kin, B.R. and Ha, S.K. (2007), "Numerical evaluation of shear strengthening performance of CFRP sheets/strips and sprayed epoxy coating repair systems", *Compos. Part B - Eng.*, **39**, 851-862.
- Lee, J. and Fenves, G.L. (1998), "Plastic-damage model for cyclic loading of concrete structures", *J. Eng. Mech. - ASCE*, **124**(8), 892-900.
- Lourenço, P.B., Rots, G. and Blaauwendraad, J. (1998), "Continuum model for masonry: Parameter estimation and validation", *J. Struct. Eng. - ASCE*, **124**(6), 642-652.
- Lubliner, J. Oliver, J. Oller, S. and Oñate, E. (1989), "A Plastic-Damage Model for Concrete", *Int. J. Solids Struct.*, **25**, 299-329.
- Maekawa, K., Pimanmas, A. and Okamura, H. (2003), *Nonlinear mechanics of reinforced concrete*, Spon Press.
- Nateghi, A.F. and Alemi, F. (2008), "Experimental study of seismic behavior of typical Iranian URM brick

- walls”, *Proceedings of the 14th World Conference on Earthquake Engineering*, Beijing, China, October.
- Oshima, M. and Hashimoto, C. (1984), “Mechanical properties of concrete confined by steel rings”, *In Summaries of the 39th annual convention*, Japan Society of Civil Engineers, Vol. V.
- Oyarzo-Vera, C., Abdul Razak, A.K. and Chouw, N. (2009), “Modal testing of an unreinforced masonry house”, *International Operational Modal Analysis Conference*, Portonovo, Ancona, Italy.
- Page, A.W. (1983), “The strength of brick masonry under biaxial compression-tension”, *Int. J. Masonry Cosntr.*, **3**(1), 26-31.
- Pillai, S.U. and Menon, D. (2010), *Reinforced concrete design*, Tata McGraw-Hill Education Private Limited, New Delhi, India.
- Rai, D.C., Agnihotri, P. and Singhal, V. (2011), “Out-of –plane strength of damaged unreinforced masonry walls”, *Proceedings of the 12th North American Masonry Conference*, Minneapolis, Minnesota, USA.
- Simulia, D.S. (2011), *Abaqus/CAE user's manual*, Providence, RI.
- Vecchio, F.J. (1990), “Reinforced concrete membrane element formulation”, *J. Struct. Eng. - ASCE*, **116**(3), 730-750.
- Zhuge, Y., Thambiratnam, D. and Corderoy, J. (1998), “Nonlinear dynamic analysis of unreinforced masonry”, *J. Struct. Eng. - ASCE*, **124**(3), 270-7.